

# **Synthesis of Attrition Resistant Fe Catalysts Using Templated Mesoporous Silica**

Hien N. Pham, Magnus Bergroth and Abhaya K. Datye

Center for Microengineered Materials and Department of Chemical & Nuclear Engineering, University of New Mexico, Albuquerque, NM 87131

## **Abstract**

A novel approach has been developed to synthesize attrition resistant heterogeneous catalysts using templated mesoporous silica. This technique makes use of a liquid-crystal template mechanism to create a silica structure where high loadings of iron oxide nanoparticles are trapped inside. The structure provides controlled porosity for transport of reactants and products to the catalytically active phase. By encapsulating the catalytically active phase, we prevent attrition of the catalyst particles as iron oxide undergoes phase changes in a reactor. Spray pyrolysis provides a rapid, inexpensive process for the synthesis of encapsulated catalysts ranging from sub-micron to tens of micron in diameter. These catalysts are suited to the Fischer-Tropsch (F-T) synthesis where the attrition of the catalytically active phase hinders performance. This method may be applicable to other mesoporous materials and active phase combinations.

## **Introduction**

This work is directed towards developing a novel approach to the synthesis of heterogeneous catalyst particles encapsulated in a templated mesoporous silica. We make use of a liquid-crystal template mechanism to create a silica shell whereby nanosized particles are trapped inside the shell. The silica shell acts as a filter to allow

gas to diffuse inside the shell for reaction to proceed, while keeping the catalyst nanoparticles inside the shell.

Our proposed technique of catalyst synthesis is novel in that it makes use of liquid-crystal templates to produce controlled porosity. The porous matrix is synthesized using silica, but the approach can be extended to other catalytic supports such as titania, zirconia or alumina. The proposed catalyst synthesis may be particularly attractive for F-T synthesis, a process used to convert energy reserves of coal and natural gas into liquid transportation fuels, using a slurry phase bubble column reactor (SBCR). The SBCR involves the suspension of the catalyst particles in a hydrocarbon oil slurry, while the gas phase reactants are bubbled through the slurry. If the catalyst undergoes attrition and generates fine particles, separation of the hydrocarbon wax products becomes difficult, particularly when nanosized particles are formed from the catalyst. The filter system can become plugged by the submicron and smaller sized particles. In the proposed technique, attrition is minimized by keeping the catalyst particles inside an attrition resistant shell.

In a previous study [1], we have explored the role of binder morphologies to provide improved attrition resistance for Fe F-T catalysts. Using the ultrasonic fragmentation approach [2,3], we found that a precipitated Fe-Cu catalyst, as-prepared, was weak compared to the same catalyst, which was spray-dried. Spray-drying improved the attrition resistance of the catalyst. The role of silica binder addition and calcination was then explored to increase the attrition resistance, and the synthesized catalysts were compared to a VISTA alumina. Results showed that the spray-dried catalyst containing silica was the best amongst the synthesized Fe F-T catalysts. Also, we investigated factors that determined the strength of our catalysts. We concluded that particle

morphology was an important parameter dependent on strength. The precipitated silica was found to provide a morphology that was suitable for holding together the primary catalyst particles.

Even though the spray-dried catalyst containing precipitated silica is attrition resistant, the pores are randomly distributed. With our novel approach, we can obtain a more narrow distribution of pore size and control the porosity of silica. Obtaining a narrow distribution of pore size may be beneficial to certain catalytic applications where the size may limit the range of products that can be formed due to diffusion limitations.

The synthesis of mesoporous materials has attracted great interest in the field of catalysis, biomaterials, membrane and separation technology, and molecular engineering. However, some mesoporous materials, such as silica, are invariably amorphous, with pores that are irregularly spaced and broadly distributed in size [4,5]. Recently, mesoporous silica has been synthesized by means of a liquid-crystal template mechanism, in which the silicate material forms inorganic walls between ordered surfactant micelles. Kresge et al. [6] first described the synthesis of mesoporous silica by means of a liquid-crystal template mechanism, in which the silicate material forms inorganic walls between ordered surfactant micelles. Ordered arrays of cylindrical micelles are formed, with the silicate species occupying the space between the micelles. Once an ordered array of uniform channels is established, the original organic material can be burnt off to produce a stable mesoporous molecular sieve.

Göltner et al. [7] used the liquid crystal phase to form ordered mesoporous silica, where the sol-gel synthesis of the inorganic nanostructure took place in the ordered environment of a bulk surfactant mesophase. Beck et al. [8] described a new family of

mesoporous molecular sieves prepared with liquid crystal templates. One member of this family, MCM-41, was characterized as hexagonal, with uniform and controllable pore size from  $\sim 15 \text{ \AA}$  to  $> 100 \text{ \AA}$ , high surface area, and high hydrocarbon sorption capacity. Other members, such as those exhibiting cubic symmetry, have been synthesized. Schulz-Ekloff et al. [9] developed a new procedure based on the precipitation of MCM-41 particles due to a gradual decrease in pH, enabling control of the morphology of mesoporous molecular sieves. Both ordering and worm-like morphologies of the mesoporous silica were formed. The consistency of the structure parameters determined by physically differing methods was checked using a geometrical model of the honeycomb structure.

Behrens *et al.* [10] and Monnier et al. [11] reported that mixtures of CTAB/silica precursor/water at low pH and low surfactant concentration ( $\sim 1 \text{ wt.}\%$ ) produced mesoporous solid precipitates. Attard et al. [12] showed that hexagonal mesophases were obtained at higher CTAB/water ratios ( $\sim 50 \text{ wt.}\%$ ). Also, in the case of low pH and low surfactant concentration, three factors were proposed for successful templating: multidentate binding of positively charged silicate oligomers to surfactant molecules via an anion, polymerization of inorganic species at the interface, and charge-density matching at the interface [11]. However, these factors were independent in the formation of mesostructures at high surfactant concentrations. Instead of using a cationic surfactant such as CTAB, Bagshaw et al. [13] used a nonionic polyethylene oxide surfactant as a template to form mesoporous molecular sieves. Disordered channel structures were obtained by varying the size and structure of the surfactant molecules.

Bergna [14] showed that attrition resistance could be conferred to catalyst particles if they were embedded in a continuous framework or skeleton of a hard and relatively inert material. This approach required the fraction of the hard phase volume to be nearly 50% to form an attrition resistant continuous framework within the grain pores. By using sub-colloidal or very small colloidal particles capable of coalescing or sintering to form a hard egg-shell, attrition resistance could also be conferred with smaller amounts (10%) of the hard phase (silica). In this case, the silica needed to be distributed on the periphery of the particles, which could be achieved by ensuring that the silica was not agglomerated during spray-drying, and that the silica particles migrated easily to the surface.

The synthesis proposed by Kresge et al. [6] involved placing a mixture of reagents in an autoclave for 48 hours. From an application standpoint, the synthesis approach would not be suitable for large-scale production. An alternative approach was described by Lu et al. [15] where they used an aerosol process for the synthesis of mesostructured spherical nanoparticles. Their methodology involves evaporation-induced surfactant self-assembly to synthesize silica thin films, membranes, particles, and nano-composite materials with highly ordered mesophase structures via dip coating or aerosol processes. A similar evaporation approach was also reported by Bruinsma et al. [16] to yield mesoporous silica. In this latter work, the authors spray-dried powders, using a precursor solution comprised of cetyltrimethylammonium chloride, hydrochloric acid, tetraethoxysilane, and water. These spray-dried mesoporous powders had structures ranging from hollow spheres to collapsed particles. Particle morphology was dependent on the precursor solution composition and drying conditions.

In this study, we examine the attrition resistance, morphology and extent of reducibility of the product material. Techniques such as ultrasonic fragmentation, pore size distribution, X-ray diffraction (XRD), transmission electron microscopy (TEM), and scanning electron microscopy (SEM) were used for the analysis. Some of the catalyst samples were studied using cross-section TEM, which was recently applied to the study of Fe F-T catalysts [17].

## **Experimental**

A precipitated Fe-Cu catalyst (64.80% Fe, 6.24% Cu by ICP based on dried weight) in its wet form (labeled PRFECU-ED20-124) was used for the experiments. The starting materials were the nitrates of Fe and Cu, and  $\text{NH}_4\text{OH}$ . Solutions of Fe-Cu nitrate and  $\text{NH}_4\text{OH}$  were mixed at  $80^\circ\text{C}$  in a continuous flow through mixer, causing the iron oxide to precipitate out. The product catalyst was discarded until the pH was between 6.8 and 7.2. The catalyst was then collected in a filter funnel, and the filter cake was pumped down to being wet but not cracked. Samples of the filtrate were obtained; a pH and brown ring test were performed for each sample to ensure that the pH remained near 7.0 and that traces of nitrate ions were removed from the catalyst, respectively. The cake was removed and then re-suspended in hot water. After filtering the slurry, samples of the filtrate were obtained for pH and brown ring testings. After the brown ring test was negative, the filter cake was pumped moist. Finally, once the precipitated Fe-Cu catalyst was dry enough to remove it off the filter, the catalyst was suspended in deionized water.

In a typical run, 100 ml of the precipitated Fe-Cu catalyst was ultrasonicated at an amplitude of 20 for 2 min to break up any loose agglomerates. The sample was then

mixed with a templated silica precursor consisting of 5 g cetyltrimethylammonium bromide (CTAB; Aldrich), 2 ml HCl (1N; J.T. Baker), 20 ml tetraethyl orthosilicate (TEOS; Aldrich), and 100 ml deionized water. More deionized water was added to prepare 250 ml of slurry, and the mixture was spray-dried using a Buchi 190 Mini Spray Dryer. The inlet temperature of the spray dryer was over 200°C with the outlet being maintained over 100°C. The product was calcined in air at 400°C for 4 hr to remove the CTAB template, thereby creating a porous structure. The catalyst was then subjected to ultrasonic energy at an amplitude setting of 20 (100 W) at 5 min intervals using a Tekmar 501 ultrasonic disrupter (20 kHz  $\pm$  50 Hz) equipped with a V1A horn and a ½” probe tip. After different extents of ultrasonic irradiation, the particle size distribution was analyzed to detect the mode of particle fragmentation.

#### *Physisorption Method*

A Micromeritics ASAP 2010 unit was used to analyze the pore size distribution of the encapsulated material. In a typical run, 0.1 g of the catalyst sample was degassed in N<sub>2</sub> at 120°C for 18 hr to remove any contaminants and moisture which may have adsorbed onto the surface of the sample. The sample was re-weighed to determine the weight loss after degassing. Nitrogen adsorption/desorption isotherm analysis was then performed at 77K for several hours.

#### *Reduction Studies*

For reduction studies, H<sub>2</sub> was obtained from Trigas, and O<sub>2</sub> and He were obtained from Argyle. The H<sub>2</sub> and He gases were further purified by passing it through an

AllTech Oxy-Trap. The reactor was a differential fixed bed reactor consisting of a stainless steel U-tube in which a known weight of catalyst was placed over a quartz wool plug. The reactor was enclosed by an electrically heated Glass-Col heating mantle, and the catalyst temperature was monitored and controlled by a thermocouple connected to an Omega PID controller. The gas flow rates were set and controlled by Tylan FC-260 mass flow controllers.

In a typical reaction run, approximately 50 mg of the sample was loaded into the reactor. The sample was initially degassed in He at 200°C for 1 hr to remove moisture or contaminants adsorbed on the surface of the sample, and then cooled back to room temperature. The sample was heated in H<sub>2</sub> from 25°C to 300°C at a rate of 10°C/min, and was reduced at 300°C overnight.

In order to passivate the sample, it was initially purged in He at 300°C for 30 min and cooled to room temperature. A very small amount of O<sub>2</sub> was introduced in the flowing He (< 1% O<sub>2</sub> in He). The oxygen was then gradually increased to a final concentration of 20% O<sub>2</sub> in He in order to simulate atmospheric conditions. Passivation was achieved when there was no further rise in temperature with an increase in O<sub>2</sub> intake. The sample was then removed for further characterization tests.

## Results

Fig. 1 shows a cumulative mass distribution plot for a precipitated Fe-Cu catalyst encapsulated in a spray-dried silica. There is attrition of particles after 5 min of ultrasonic irradiation due to fracture, as indicated by the shift in curves to the right, i.e., towards smaller size particles. However, little fracture occurs thereafter. Furthermore,

very little generation of fine particles below 6  $\mu\text{m}$  occurs after 25 min of ultrasonic irradiation due to erosion, as indicated by an increase in the percentage of fines for a particular particle size. SEM image (Fig. 2) shows that some of the particles are spherical, while others contain several dimples on their surfaces due to rupturing of the particles during the spray-drying process. A few of the particles are hollow and broken as seen in the SEM image. This is due to the formation of a rigid crust by premature solidification of silica. Furthermore, because the wall of the crust is thin, the particles break down easily due to particle-particle collision, particle-wall collision or handling of the dry powder. The majority of the particles are dense, as seen in the TEM images below.

TEM image (Fig. 3) shows the precipitated Fe-Cu catalyst particles, with an average size of 80 nm, are uniformly distributed within the silica. Furthermore, the nanoparticles appear to be almost completely encapsulated inside the spray-dried mesoporous silica. This is clarified by X-ray Photoelectron Spectroscopy, where the surface compositions of the Fe and Si elements are 3.45 wt.% and 55.25 wt.%, respectively. The surface composition is much less than the bulk composition, indicating that the iron phase is distributed preferentially in the interior of the particles. Fig. 4 shows a higher magnification view. From this image, it is difficult to interpret the actual internal microstructure of the encapsulated material. Hence, cross-sectioning was performed to investigate the internal microstructure.

Fig. 5 shows a XTEM image of an encapsulated particle. The image shows that we can disperse a high loading of precipitated Fe-Cu catalyst, within the mesoporous silica. Fig. 6 shows a XTEM image of this particle at a higher magnification. In this

image, the ordered pore structure in the silica phase can be clearly seen to be preserved all around the iron nanoparticles. Fig. 7 shows another XTEM image where the crystalline particles are surrounded by mesoporous silica. The internal microstructure does not involve a silica shell that encapsulates the catalyst particles. Rather, the iron particles seem to be uniformly distributed throughout the spray-dried particle. Fig. 8 shows a XTEM image of a larger particle. The area near the surface of the encapsulated particle is similar to a spray-dried silica shell (not shown), whereby there are ordered pore structures. Internally, there appears to be a mixture of both ordered and less ordered silica structures, yet does not involve the silica shell, as seen by the image in Fig. 7.

Fig. 9 is a  $N_2$  adsorption/desorption isotherm curves for the encapsulated material. The curves show hysteresis, indicating that a multi-dispersed phase is present. BJH pore size distribution plot (Fig. 10) shows three peaks. The peak at  $\sim 23 \text{ \AA}$  corresponds to the ordered mesoporous silica shell. The other two peaks at  $\sim 50 \text{ \AA}$  and  $\sim 150 \text{ \AA}$  correspond to the less ordered structures inside the silica shell.

Fig. 11 shows XRD plots for the encapsulated material, before and after reduction. Before reduction, the precipitated Fe-Cu catalyst is determined to be hematite ( $\alpha\text{-Fe}_2\text{O}_3$ ) with copper as a promoter. After reduction, there are no peaks corresponding to hematite. Instead, hematite has been reduced to  $\alpha\text{-Fe}$ . Silica does not appear to affect the reducibility of the catalyst. The pores of the silica are large enough to allow catalyst accessibility to the gas phase, while the nanoparticles are maintained inside the silica structure. This experiment shows that the iron phase is completely reducible in  $H_2$ , as determined by XRD. Reduction of the iron oxide is a necessary step in making it active as a F-T catalyst.

## Discussion

In a previous study [1], we have shown that a precipitated silica improved the attrition resistance of Fe F-T catalysts. Further analyses of pore size distribution—not shown in our previous paper—showed that the catalysts containing precipitated silica has a broad distribution of pore sizes. This type of pore size distribution may limit the selectivity of hydrocarbon products due to diffusion limitations. By obtaining a much narrower pore size distribution, the encapsulated material allows for far greater selectivity of hydrocarbon products, which results in a more tightly controlled reaction with fewer by products. The ordered pore structure also allows facile transport of reactants and products to the catalytically active sites.

Bergna' s method for preparing attrition resistant catalysts [13] may not be entirely suitable for catalysts which undergo phase transformations during their use. For example, as shown by Shroff et al. [18], iron catalysts start out in the form of an oxide and get converted to an iron carbide after activation in a F-T reaction environment. The changes in density between the oxide and carbide phase leads to a break-up of the iron oxide to form nanoparticles of iron carbide. Hence, even if the catalyst could be prepared in attrition resistant form, the phase changes may tend to weaken the catalyst during use. In our method, the iron particles could be retained from this phase transformation within the silica structure.

The method by Bruinsma et al. [15] yielded hollow silica shells when liquid droplets were spray-dried. The hollow shells could be easily crushed and would not provide any attrition resistance, especially if the shell wall was too thin to maintain its

strength. We have shown that the encapsulated material consisted of a silica shell filled iron nanoparticles. By producing a more solid structure, this material possesses the desired attrition resistance properties, as shown by the cumulative mass distribution plot in Fig. 1. Attrition of the catalyst particles is minimized since the active phase crystallites are encapsulated inside an attrition resistant mesoporous silica shell.

In many applications where high loadings of the dispersed phase are required, impregnating a mesoporous support with a catalytically active metal will result in non-spherical particles. With our method, we can produce more spherically shaped particles with high loadings of the dispersed phase. The spherical shape of the particles may be important for proper slurry hydrodynamics, such as in a bubble column reactor. For example, during operation of stirred tank reactor, more attrition would be expected with non-spherical particles than with smooth spherical particles.

In addition to attrition testing and characterization, we have shown that by reducing in hydrogen at 300°C, the iron oxide, hematite, could be completely reduced to metallic iron. Usually, silica tends to decrease the catalytic activity of Fe F-T catalysts. In this case, silica does not affect reducibility of the catalyst. The supporting structure of the encapsulated material appears to retain the nanoparticles, yet at the same time it provides access to the catalytic sites to the reactants and easy egress of the products of reaction. In future work, we plan to study the reduction of the encapsulated material in syngas ( $H_2/CO = 0.7$ ) and to determine the reactivity under F-T synthesis conditions.

## Summary

We have developed a novel approach to the synthesis of attrition resistant heterogeneous catalysts using a templated mesoporous silica. This technique makes use of a liquid-crystal template mechanism to create a silica structure where nanoparticles are trapped inside. Ultrasonic fragmentation followed by particle size distribution measurements was used to characterize the strength of this material. It was found that there was attrition due to fracture (as the hollow shells break up) after 5 min of ultrasonic irradiation, but little fracture occurred thereafter. Also, very little generation of fine particles below 6  $\mu\text{m}$  occurred after 25 min of ultrasonic irradiation. A few of the particles were hollow due to premature solidification of silica and therefore broke up easily, but the majority of the particles were dense.

From TEM, the catalyst particles were uniformly distributed within the silica and were almost completely encapsulated inside the silica shell. Using cross-sectioning, we could confirm that a high loading of catalyst was present within the mesoporous silica structure. From pore size distribution, three peaks were present: one peak at a small pore size corresponded to the ordered mesoporous silica shell and the two peaks at higher pore sizes corresponded to the less ordered structures inside the shell.

Finally, XRD showed that the Fe catalyst, determined to be hematite, was reduced to metallic iron in hydrogen. Silica did not appear to affect the reducibility of the catalyst. Furthermore, the pores of the silica were large enough to allow catalyst accessibility to the gas phase. Reduction of the encapsulated material in syngas will be the subject of future work.

## References

- [1] H.N. Pham, A. Viergutz, R.J. Gormley, A.K. Datye, "Measuring the Attrition Resistance of Slurry Phase Heterogeneous Catalysts", *Powder Technology*, in press.
- [2] S.G. Thoma, M. Ciftcioglu, D.M. Smith, *Powder Technol.* 68 (1991) 53.
- [3] S.G. Thoma, M. Ciftcioglu, D.M. Smith, *Powder Technol.* 68 (1991) 71.
- [4] T.J. Pinnavaia, *Science* 220 (1983) 365.
- [5] R.M. Tindwa, D.K. Ellis, G.Z. Peng, A. Clearfield, *J. Chem. Soc. Faraday Trans 1.* 81 (1985) 545.
- [6] C.T. Kresge, M.E. Leonowicz, W.J. Roth, J.C. Vartuli, J.S. Beck, *Nature* 359 (1992) 710.
- [7] C.G. Göltner, S. Henke, M.C. Weissenberger, M. Antonietti, *Angew. Chem. Int. Ed. Engl.* 37 (1998) 613.
- [8] J.S. Beck, J.C. Vartuli, W.J. Roth, M.E. Leonowicz, C.T. Kresge, K.D. Schmitt, C. T-W Chu, D.H. Olson, E.W. Sheppard, S.B. McCullen, J.B. Higgins, J.L. Schlenker, *J. Am. Chem. Soc.* 114 (1992) 10834.
- [9] G. Schulz-Ekloff, J. Rathouský, A. Zúkal, *Micr. Meso. Mater.* 27 (1999) 273.
- [10] P. Behrens, G.D. Stucky, *Angew. Chem. Int. Ed. Engl.* 32 (1993) 696.
- [11] A. Monnier, F. Schüth, Q. Huo, D. Kumar, D. Margolese, R.S. Maxwell, G.D. Stucky, M. Krishnamurty, P. Petroff, A. Firouzi, M. Janicke, *Science* 261 (1993) 1299.
- [12] G.S. Attard, J.C. Glyde, C.G. Göltner, *Nature* 378 (1995) 366.
- [13] S.A. Bagshaw, E. Prouzet, T.J. Pinnavaia, *Science* 269 (1995) 1242.

- [14] H.E. Bergna, *Characterization and Catalyst Development: An Interactive Approach*, American Chemical Society, 1989, pp. 55-64.
- [15] Y. Lu, H. Fan, A. Stump, T.L. Ward, T. Rieker, C.J. Brinker, *Nature* 398 (1999) 223.
- [16] P.J. Bruinsma, A.Y. Kim, J. Liu, S. Baskaran, S., *Chem. Mater.* 9 (1997) 2507.
- [17] Y. Jin, *Phase Transformations of Iron-Based Catalysts for Fischer-Tropsch Synthesis*, Dissertation, University of New Mexico, Spring, 1999.
- [18] M.D. Shroff, D.S. Kalakkad, K.E. Coulter, S.D. Köhler, M.S. Harrington, N.B. Jackson, A.G. Sault, A.K. Datye, *J. Catal.* 156 (1995) 185.

PRFECU-ED20-124 + SiO<sub>2</sub>  
Amplitude=20

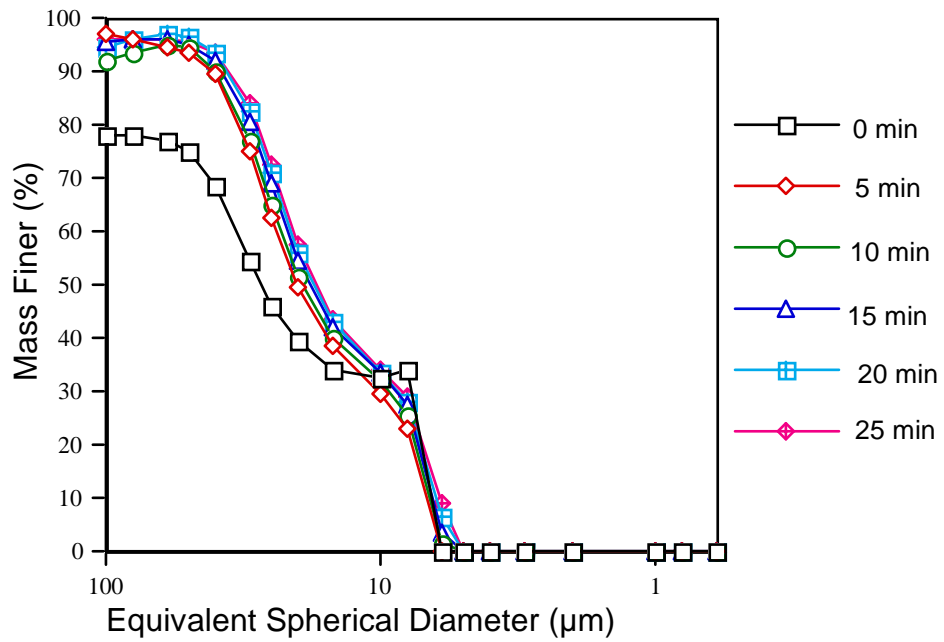


Fig. 1. Sedigraph particle size distribution of precipitated Fe-Cu catalyst particles encapsulated in spray-dried silica as function of ultrasonic irradiation. The median size is 28µm. The shift in the median size after 5 minutes is caused by the break up of hollow shells. No fracture or erosion is seen after this initial break up.

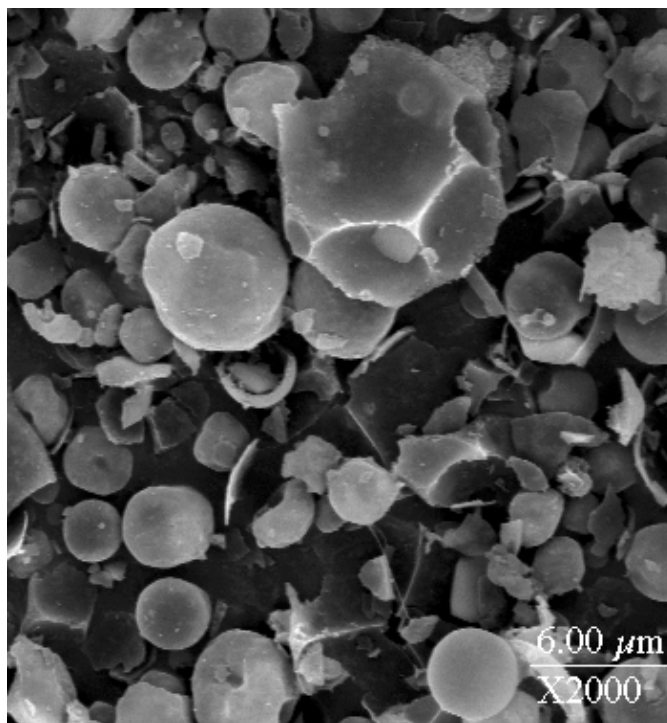


Fig. 2. SEM image of precipitated Fe-Cu catalyst particles encapsulated in spray-dried silica. A few of the particles are hollow and broken, but the majority of the particles are dense.

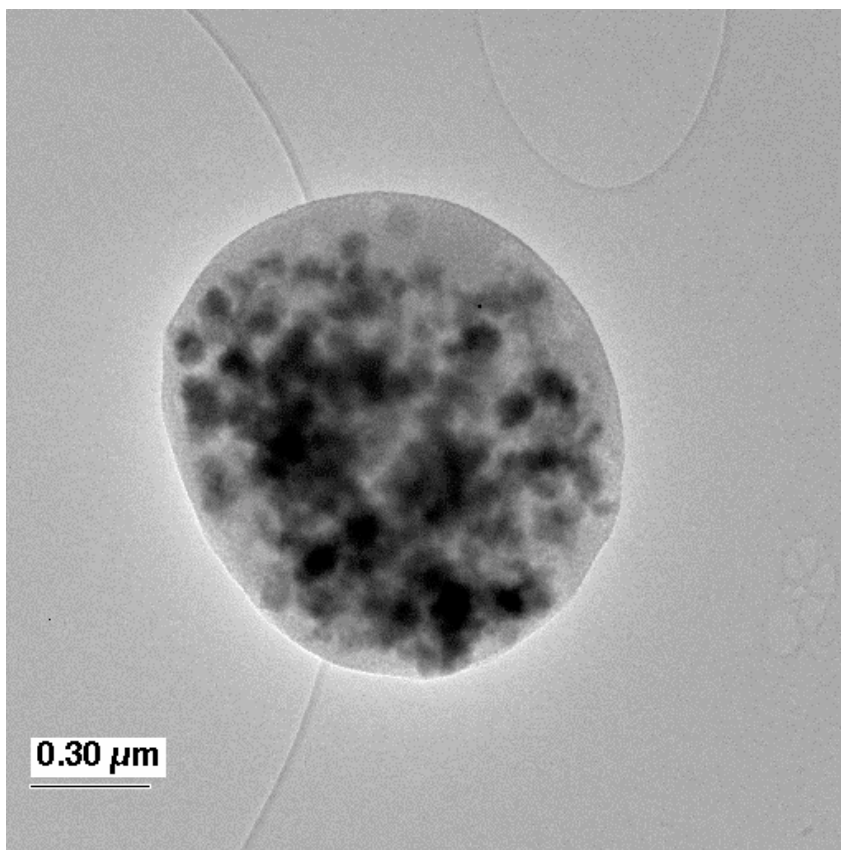


Fig. 3. TEM image of precipitated Fe-Cu catalyst particles uniformly distributed within the silica.

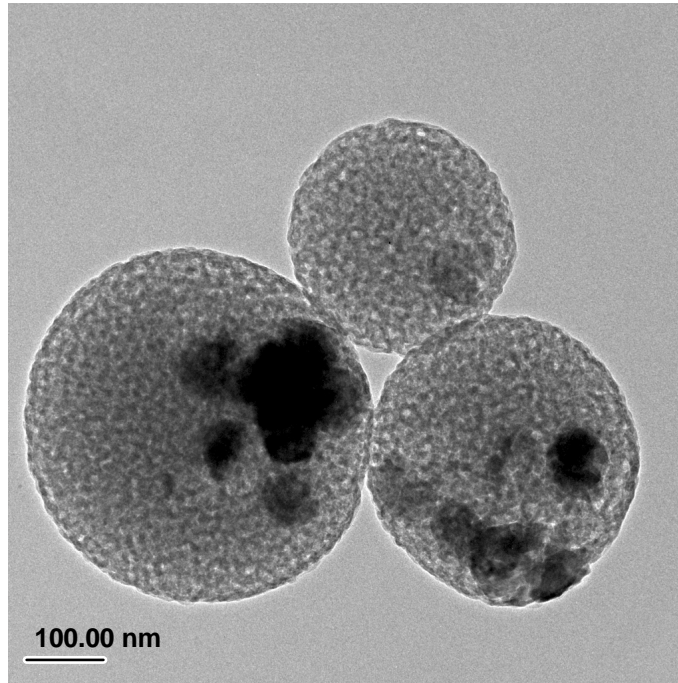


Fig. 4. Cross section TEM image of particles at a higher magnification view.

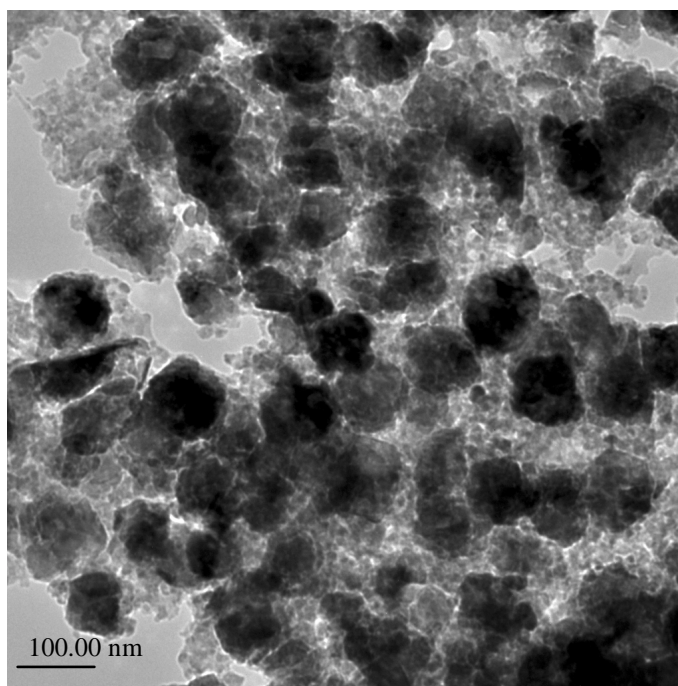


Fig. 5. Cross section TEM image shows a high loading of precipitated Fe-Cu catalyst particles dispersed within the mesoporous silica.

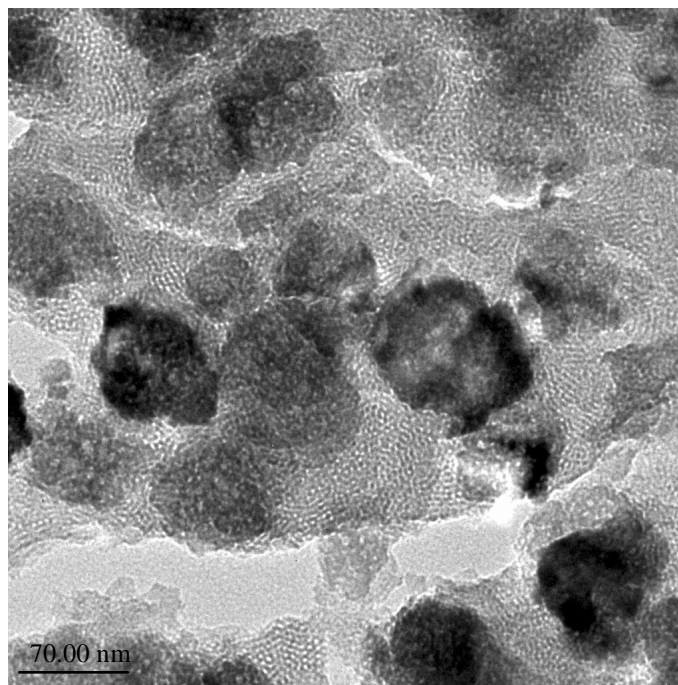


Fig. 6. Cross section TEM image of Fig. 5 at a higher magnification. The ordered pore structure in the silica phase is preserved all around the iron nanoparticles.

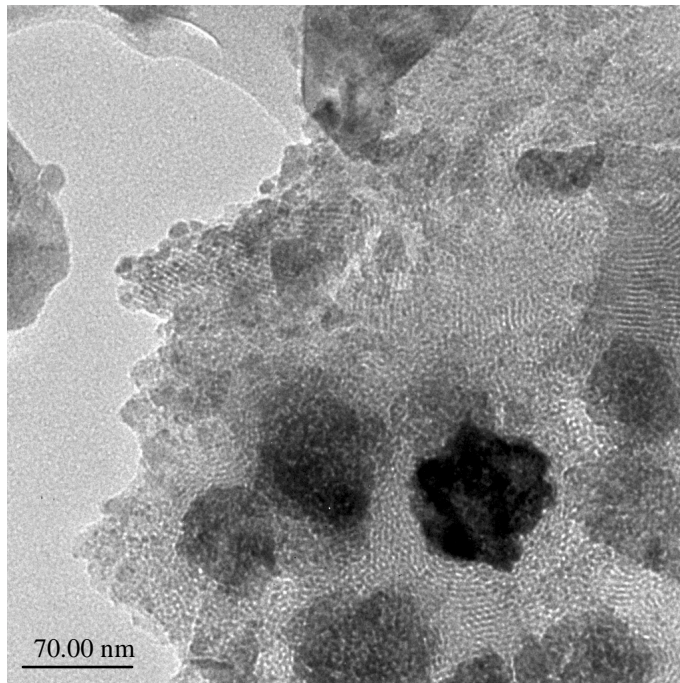


Fig. 7. Another cross section TEM image where the crystalline particles are surrounded by mesoporous silica.

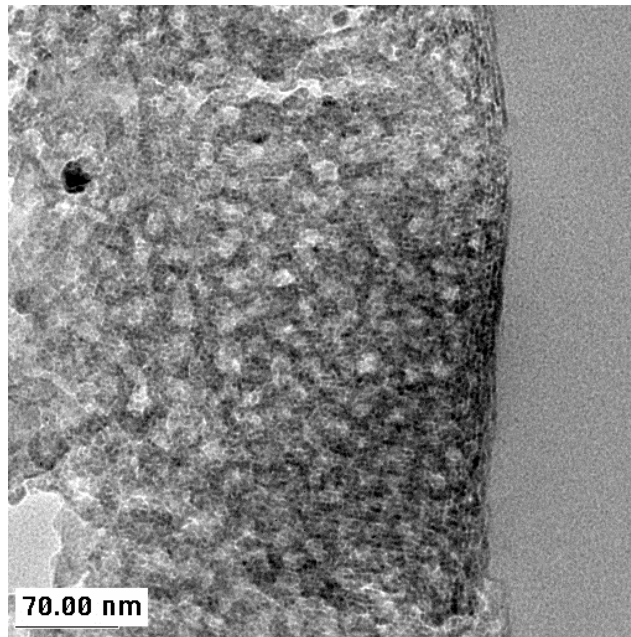


Fig. 8. Cross section TEM image shows that the area near the surface may constitute the silica shell, with very few Fe-Cu particles. Most of the iron oxide is located in the interior of the silica spray dried particles.

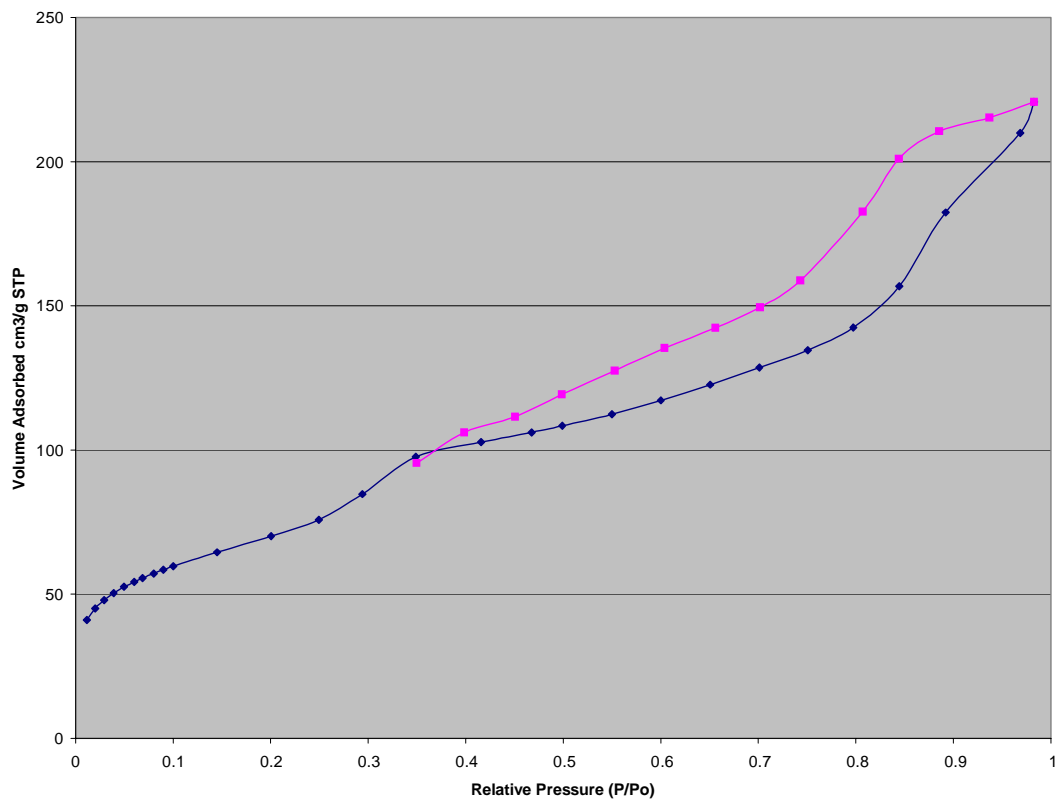


Fig. 9. Nitrogen adsorption/desorption isotherm curves for the encapsulated iron oxide in silica catalyst. The hysteresis in this curve indicates a range of pore sizes are present, as shown in the next figure.

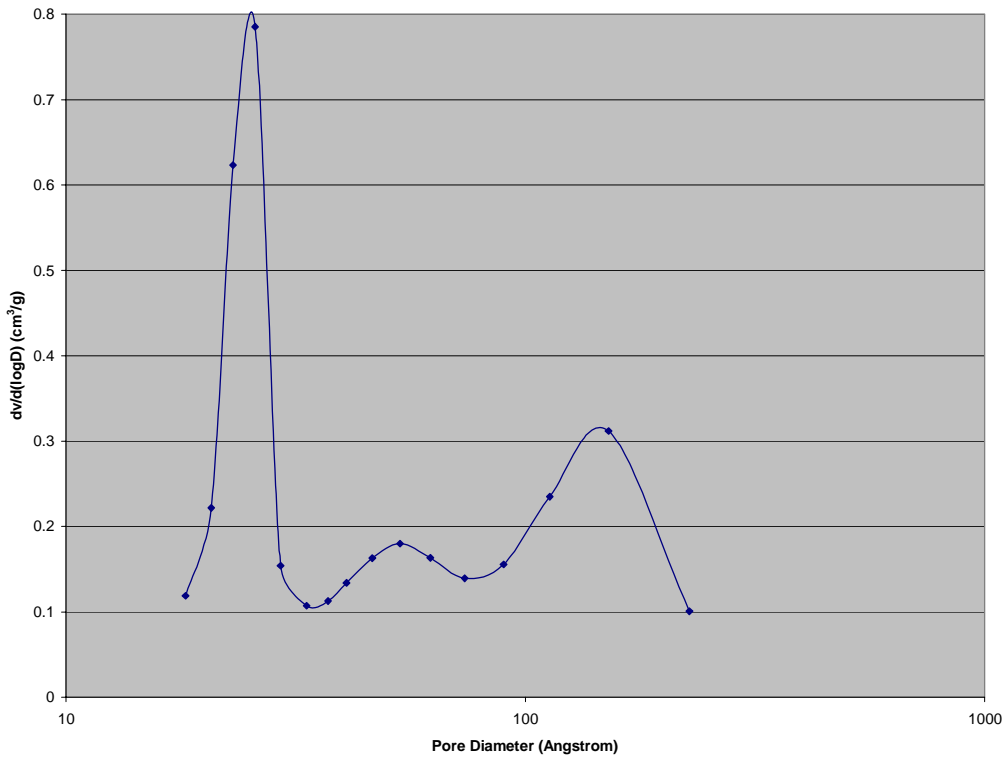


Fig. 10. BJH pore-size distribution plot from the adsorption data in Fig. 9 shows three peaks: the first peak corresponding to the ordered mesoporous silica, and the other two peaks corresponding to the internal microstructure where iron oxide particles are encapsulated in the silica shells.

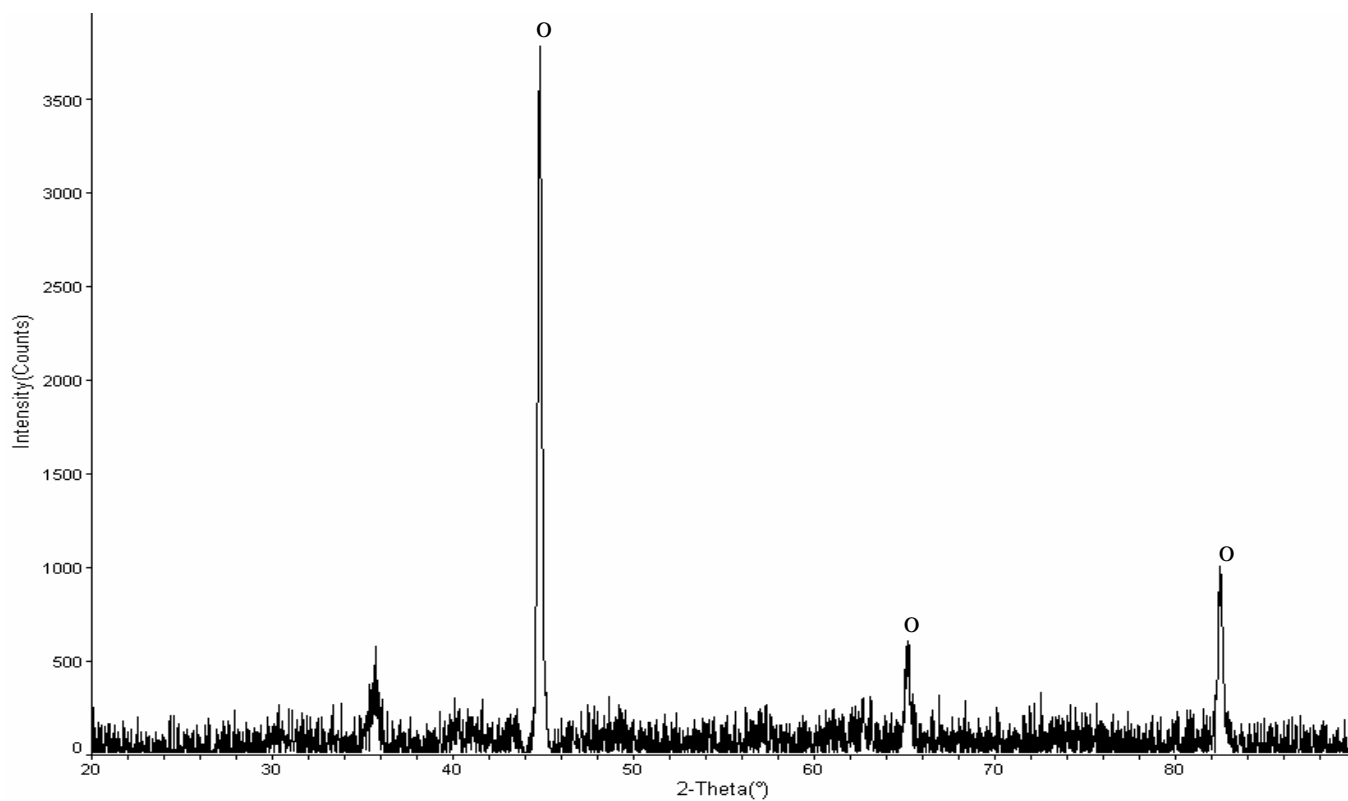
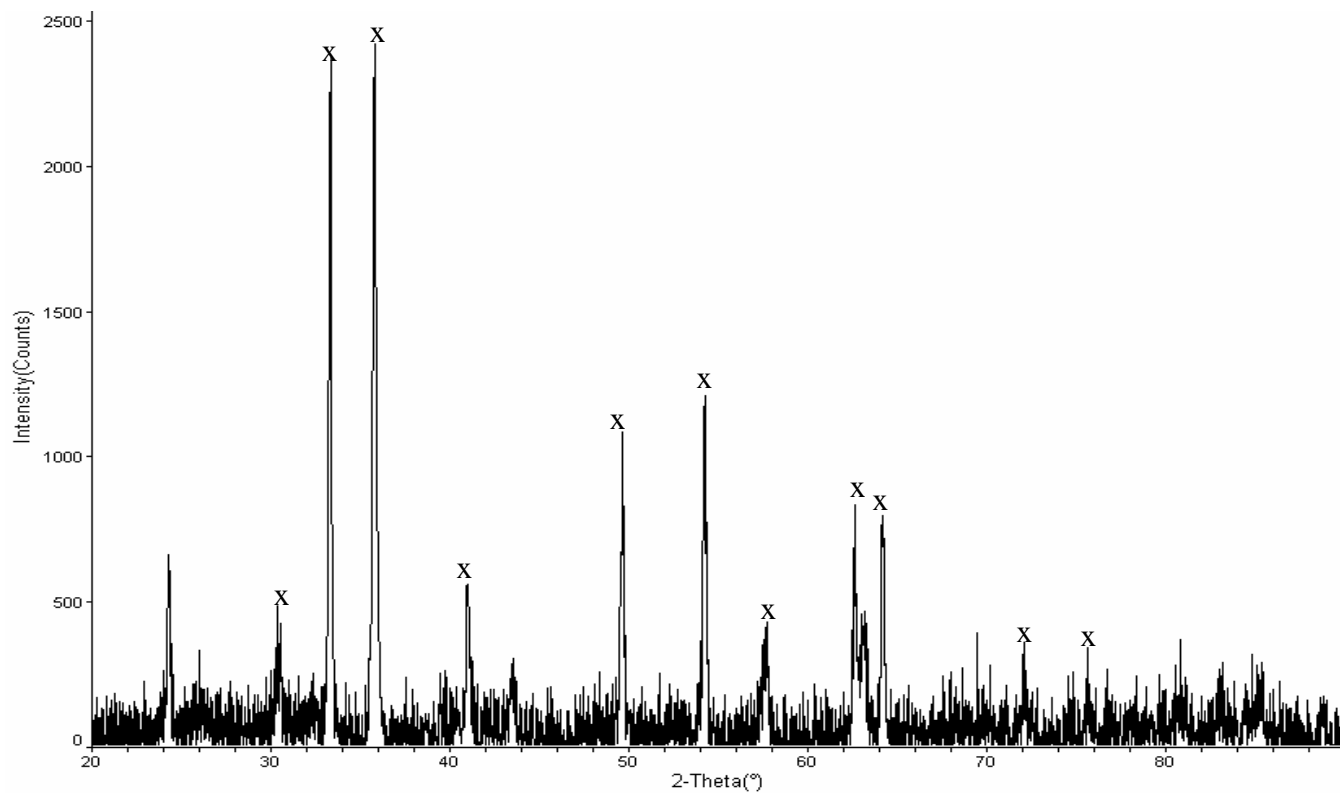


Fig. 11. XRD patterns show that the catalyst is completely reducible in hydrogen at 300 °C. Silica does not appear to affect the reducibility of the catalyst. x = hematite ( $\alpha\text{-Fe}_2\text{O}_3$ ), o = metallic iron ( $\alpha\text{-Fe}$ )